22. SIGNIFICANCE OF CLAY MINERALOGICAL AND GEOCHEMICAL DATA, WALVIS RIDGE, SOUTHEAST ATLANTIC, LEG 75, DEEP SEA DRILLING PROJECT[1]

Henri Maillot, Sédimentologie et Géochimie, E.R.A. C.N.R.S. 764, Université de Lille I—59655 Villeneuve
d'Ascq Cedex, France
and
Christian Robert, Géologie Marine, L.A. C.N.R.S. 41, Faculté des Sciences de Luminy,
13288 Marseille Cedex 9, France

ABSTRACT

Clay mineralogical and inorganic geochemical data give information on the evolution of both continental and marine paleoenvironments from late Albian to Pleistocene time. Specifically, the data indicate that: deposition of black shales occurred in an euxinic basin bounded by flat continental lowlands; that oxidation of the oceanic environment began during the Coniacian; that, from the Santonian to the Eocene, sediments were influenced by tectonic events and subsidence on the Walvis Ridge and on the African margin, as well as by the progressive deepening of the seafloor; that influences of the global climate cooling were present from early Miocene onwards; and that the development of the Benguela current system influenced sedimentation (since the Miocene principally). Fluctuations of the CCD were also determined.

INTRODUCTION

During Leg 75 of the Deep Sea Drilling Project (DSDP) two sites were drilled on the Walvis Ridge and in the Angola Basin (Fig. 1). The sediments recovered range from late Albian to late Pleistocene. Site characteristics are summarized in Table 1.

The purpose of this study is to reconstruct the paleoenvironmental conditions in the region under consideration, as indicated by clay mineralogical and inorganic geochemical variations. Similar approaches have been used previously to determine the following aspects of the paleoenvironmental evolution of the South Atlantic:

1) Formation of the South Atlantic basins (Maillot, 1979; Robert et al., 1979; Maillot, 1980; Maillot and Robert, 1980) and paleoenvironmental conditions during deposition of black shales (Chamley and Robert, 1982).

2) Cretaceous/Tertiary boundary events on the Atlantic margins (Chamley and Robert, 1979), on the Rio Grande Rise (Robert, 1981), and on the Walvis Ridge (Chamley et al., in press).

3) Cenozoic changes in climates and currents in the South Atlantic (Maillot and Robert, 1980; Robert, 1980; Maillot and Robert, in press).

4) Paleoenvironmental changes on the Falkland plateau from late Jurassic to Pleistocene (Robert and Maillot, in press).

METHODS

Clay Mineralogy

The study involved the analysis of 232 samples. In each, the sediment fraction <63 μm was decalcified in 0.2 N hydrochloric acid. The excess acid was removed by repeated centrifugations followed by homogenization. The <2 μm fraction was separated by decantation (set-

tling time based on Stokes law); oriented aggregates were then made on glass slides. Three X-ray diffractograms were made as follows: (1) untreated sample, (2) glycolated sample, (3) sample heated for 2 hours at 490°C. A C.G.R. Theta 60 diffractometer (copper Kα radiation focused by a quartz-curved crystal monochromator) was used at scan speeds of 1°2 θ/mn, with all instrument settings kept constant. A receiving slit of 1.25 mm allowed a more precise resolution of poorly crystallized minerals.

The minerals included: chlorite, illite, irregular mixed layers (chlorite–smectite and illite–smectite), kaolinite, smectite, and attapulgite (palygorskite). Associated minerals were quartz, feldspar, cristobalite, and clinoptilolite in variable abundance.

Semiquantitative evaluations were based on peak heights and areas. The height of the 001 illite peak (glycolated sample) was taken as a reference. Compared to this value, smectite, palygorskite, and irregular mixed layers were corrected by multiplying their peak height by a factor of 1.5 to 2.5, depending on their crystallinity, whereas well-crystallized kaolinite was corrected using a factor of 0.5. Final data are given in percentages, the relative error being ±5%.

Illite crystallinity was the width, at half height, of the 001 illite peak (10 Å), on the glycolated sample. The relative abundance of smectite versus illite was obtained from the ratio of the 001 smectite (18 Å) and illite (10 Å) peaks on the glycolated sample.

Geochemistry

Samples were dried at 105°C, then ground and homogenized. Next, 0.2 g were subjected to alkaline fusion, then dissolved in HCl and diluated to 100 ml. The treatment allowed gravimetric determination of SiO_2 and spectrophotometric determination of CaO, MgO, Al_2O_3, and Fe_2O_3 (by atomic absorption). Another 2 g of each sample were submitted to fluoroperchloric treatment, then dissolved in HCl and diluted to 100 ml. The dilution was used for the colorimetric analysis of TiO_2, the spectrophotometric analysis of Na_2O and K_2O (by emission) and also of Mn, Zn, Li, Ni, Cr, Sr, Co, Cu, Pb, V, and Cd (by atomic absorption). The emission and atomic absorption apparatus was a type 503 Perkin-Elmer spectrophotometer using the following methods: (1) base solution for major elements, (2) complex synthetic solution for trace elements to which 5% of lanthanum in hydrochloric solution was added.

GENERAL RESULTS

Clay Mineralogy

Clay mineral assemblages from these sites show the absence of burial diagenetic modifications. There is nei-
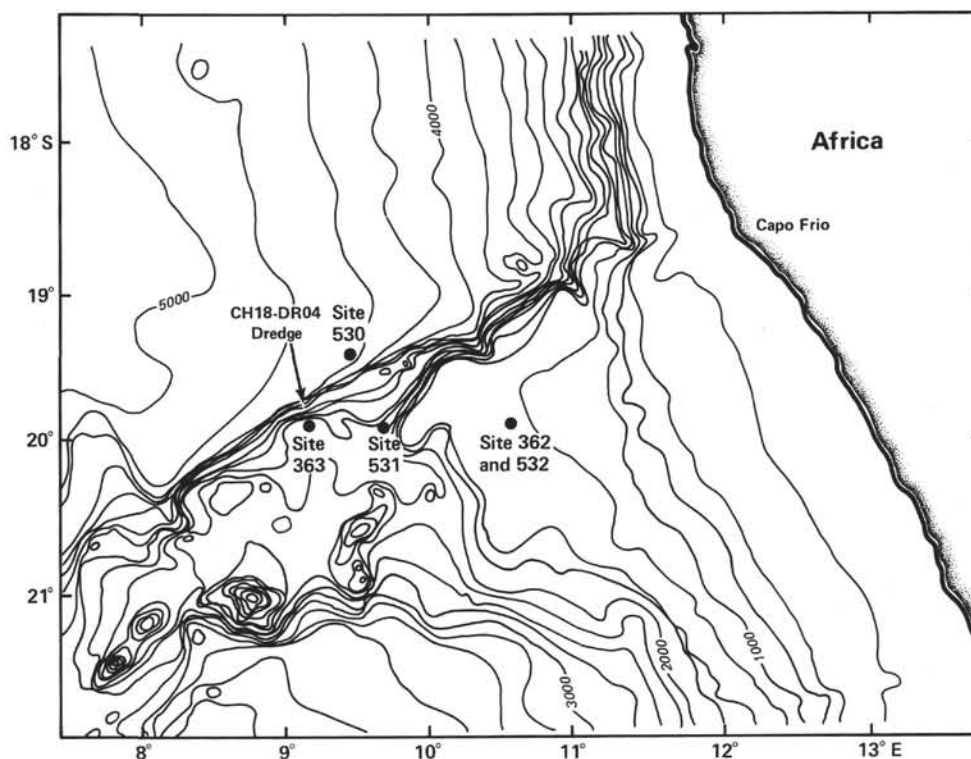

Figure 1. Site location map, Sites 362, 363 and Sites 530, 531, and 532.

Table 1. General site characteristics, Leg 75.

Site	Latitude	Longitude	Water depth (m)	Penetration (m)	Number of samples Min.	Number of samples Chem.	Oldest sediment recovered
530	19°11.26′S	9°23.15′E	4,629	1,121	168	82	late Albian
532	19°44.61′S	10°31.13′E	1,331	742	64	34	late Miocene

ther a progressive transition from smectite to mixed layers and illite, nor a reduction in illite crystallinity with increased depth at these DSDP sites. For comparison, influences of burial diagenesis on clay minerals are mentioned by Dunoyer (1969) in deeper boreholes.

Since there is no evident relationship between lithology and clay mineralogy, and since terrigenous components are abundant in these sediments, clay particles are considered to be essentially of detrital origin, formed in soils and by continental weathering as is the case in the North Atlantic (Chamley, 1979) and in other parts of the South Atlantic (Robert et al., 1979; Robert, 1981; Robert and Maillot, in press).

In Cretaceous sediments, large amounts of well-crystallized smectite, similar to the pedogenic smectite presently originating in African regions (Paquet, 1969) are present. That points to the existence of a globally warm continental climate, in agreement with the data compiled by Frakes (1979). The following aspects characterize clay mineral assemblages produced during long periods of constant warm climatic conditions (Millot, 1964; Chamley, 1979; Robert et al., 1979): (1) chlorite, illite, and mixed-layer minerals result principally from the direct erosion of rocks and from moderate continental weathering; (2) kaolinite is derived from soils developed

in sloping and well-drained upstream areas; (3) smectite comes mainly from deep soils in downstream areas of continental drainage basins, where relief is low and drainage poor; (4) palygorskite (attapulgite) is derived mainly from sediments of confined coastal basins. The Santonian to Eocene sediments recovered during Leg 75 show the increasing importance of direct erosion of rocks, moderate continental weathering, and the presence of coastal confined basins.

In Cenozoic sediments, and especially since the late Eocene, the abundance of chlorite, illite, and mixed layers increase progressively, following the general climate cooling (Chamley, 1979) and the latitudinal zonation of climates and soils (Goldberg and Griffin, 1964; Pedro, 1968). The distribution of the clay minerals in the ocean is affected by several factors, the most important being the influence of oceanic water masses and circulation (Robert, 1980). In the Plio–Pleistocene sediments of the South Atlantic, intermediate water masses are enriched in illite and mixed layers originating from temperate areas; North Atlantic Deep Water is marked by kaolinite from equatorial regions; and Antarctic Bottom Water contains an important proportion of smectite. The general climatic trend is present with fluctuations in the abundance of the minerals in the Cenozoic sediments recovered during Leg 75.

Geochemistry

In oceanic sediments, Fe and Mn accumulations originate from detritic (fine or coarse fractions), hydrogenous, biogenic, or volcanogenic sources or by diagenetic processes (Elderfield, 1977). Despite these various possible origins, it seems that the relative abundances of Fe

and Mn are significant for paleoenvironmental study (Turekian, 1965; Boström et al., 1972; Maillot, 1980; Maillot and Robert, 1980). Krashnaswami (1976) considered Fe–Mn values higher than concentrations in a typical detrital shale to indicate an authigenic influence in the sediment formation. He used the index

$$Mn^* = \log \left[\frac{Mn \; sample}{Mn \; shale} \bigg/ \frac{Fe \; sample}{Fe \; shale} \right]$$

where values of Mn shale and Fe shale are given by Boström et al. (1976). The variations in this index show the influence of oceanic basalts and oxidizing currents.

Al is principally related to the detritic minerals. An index proposed by Boström (1969, 1970) permits the recognition of detrital particles: $D^* = Al/Al + Fe + Mn$, associated with $Si^* = SiO_2/Al_2O_3$ (siltstones, sandstones). D^* is close to 0.63 in typical terrigenous shales. A decrease of D^* indicates less significant continental influence on sedimentation. Very high values of D^* sometimes correspond to abundant kaolinite particles. Si^* expresses the excess Si (i.e., not associated with Al). This silica can be from volcanogenic (ashes), biogenic (diatoms, radiolarians), or detritic (quartz) origin.

The ratios $Mg^* = MgO/Al_2O_3$ and $Fe^* = Fe_2O_3/Al_2O_3$ permit the interpretation of variations in MgO and Fe_2O_3 with respect to clay mineral abundances.

The index $Sr^* = 10^3 \; Sr/CaO$ is generally related to processes of carbonate dissolution (Maillot and Robert, 1980). When the variations related to burial diagenesis or to the primary compositions of the carbonates are mathematically determined, Sr^* confirms the processes of carbonate dissolution as inferred by others methods (Maxwell et al., 1970; van Andel et al., 1977; Melguen, 1978; Melguen et al., 1978). Three sorts of dissolution appear:

1) Very high Sr^*: This type of dissolution is present in organic rich sediments and depends on the intensity of the reduced sedimentary environment.

2) High Sr^*: In open marine and oxidizing environments, this type of dissolution appears in the vicinity of the carbonate compensation depth (CCD). High Sr^* values result from the low solubility of $SrCO_3$ compared with $CaCO_3$ (Nekrassov, 1966) or form the partial adsorption of Sr by clay minerals (Baush, 1968).

3) Low Sr^*: This type of dissolution occurs when the sediment has been deposited above the CCD.

ANGOLA BASIN, HOLES 530, 530A, 530B

Lithology (Fig. 2)

The base of the sedimentary section consists of upper Albian, Cenomanian, lower Turonian, and Coniacian/Santonian red and green claystone, and marlstone with interbedded black shales. Under this sedimentary complex, the basement consists of fine-grained basalt containing veins and vugs filled with calcite.

The Santonian to Campanian interval is represented by volcanogenic sandstone, variegated red, green, and purple claystone, siltstone, and sandstone.

The Campanian to lower Maestrichtian sediments consist of mudstone, marlstone, clastic limestone, and siliciclastic sandstone. The upper Maestrichtian to Eocene interval is represented by a multicolored mudstone, marlstone, chalk, and clastic limestone. Sediments vary from nannofossil marl and ooze, diatom ooze, and debris-flow deposits to green and red mud from late Oligocene to Pleistocene.

Clay Mineralogy (Fig. 2)

Several mineralogical units can be distinguished at this site. From late Albian to Campanian (Cores 530A-105 to 74), smectite is the major clay mineral (65 to 100%), accompanied by chlorite (0 to 10%), illite (0 to 15%), mixed-layers (0 to 10%), and palygorskite (0 to 5%). Quartz and feldspar are also present. This clay-mineral assemblage suggests a dominant influence of pedogenic detrital supply originating from flat coastal areas developed on subdued relief.

From Campanian to Eocene (Cores 530A-73 to 37), illite (0 to 50%), and palygorskite (0 to 70%) increase, while smectite (25 to 100%) decreases. Chlorite (0 to trace amounts) and mixed layers (0 to 15%) are also present, as well as quartz, cristobalite, and clinoptilolite. This clay mineral association indicates an important detrital supply from altered rocks, moderate continental weathering, and confined coastal basins. In Core 530A-72, the increase of illite (45%) is sharp and very important. The greenish volcanogenic sandstones consist of 20% glauconite. In this level, clay minerals are probably influenced by diagenetic effects that occurred during the processes of glauconitization—i.e., transformation of clay minerals and/or neoformation of illite. If one considers the pelagic environment of the site, and the formation of glauconite in shallower environments as present Atlantic shelf (Odin and Giresse, 1972), glauconite at Site 530 is certainly redeposited.

In this unit, palygorskite is present in long, straight, or flexuous fibers, suggesting its formation close to the site (Plate 1). Moreover, the presence of coalescent fibers, growing at the periphery of dense particles, suggests that palygorskite probably developed partially by transformation processes, as shown by Trauth (1976) and was then removed by erosion in the ocean.

From the late Oligocene onward (Cores 530A-37 to 2 and 530B-34 to 1), chlorite (0 to 5%), illite (trace amounts to 30%), mixed layers (0 to 20%), and kaolinite (0 to 15%) increase progressively. At the same time, the abundance of smectite (35 to 95%) diminishes and palygorskite (0 to trace amounts) disappears. Quartz and feldspar are also present. This progressive mineralogic trend is related to the Cenozoic climate cooling.

Geochemistry (Fig. 2 and Tables 2 and 3)

From Albian to Coniacian-Santonian (Cores 530A-105 to 87), the geochemical facies have the characteristics of the typical black shales described by Vine and Tourtelot (1970), Natland (1978), and Maillot (1980). C_{org}, Cu, Ni, Zn, Co, Cr, and V increase simultaneously. Mean values obtained from five samples of black
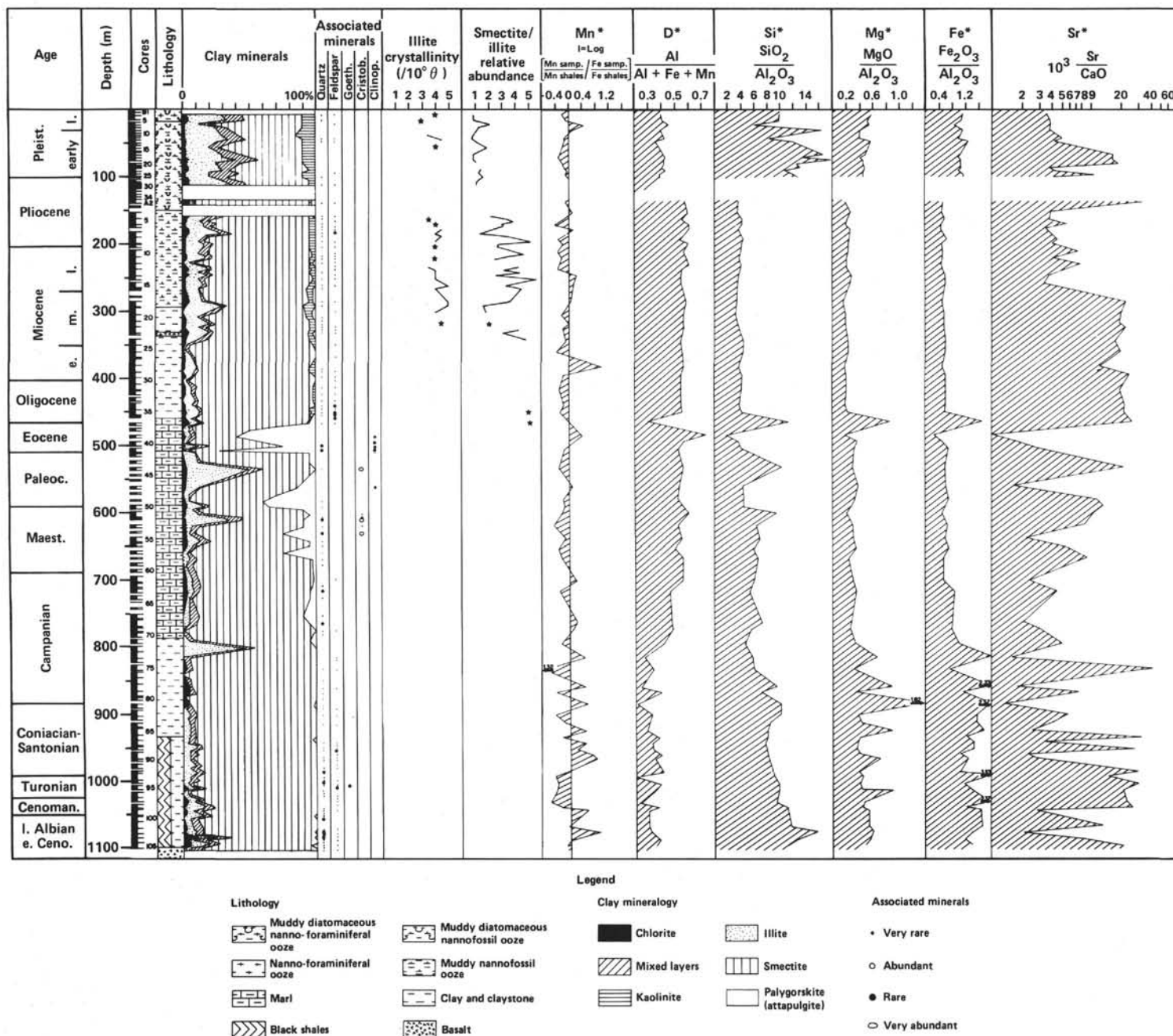
Figure 2. Lithology, geochemistry, and clay mineralogy, Site 530.

Table 2. Arithmetic means of geochemical analysis of five black shales.

Oxide	(%)	Element	(ppm)
SiO$_2$	53.44	Sr	170 ppm
Al$_2$O$_3$	6.00	Cu	178 ppm
CaO	0.73	Ni	214 ppm
MgO	2.50	Co	135 ppm
Na$_2$O	1.57	Zn	522 ppm
K$_2$O	3.12	Pb	32 ppm
TiO$_2$	1.14	V	380 ppm
Fe$_2$O$_3$	10.95	Cr	175 ppm

shales (Samples 530A-89-4, 52 cm, 93-5, 26 cm, 94-1, 43 cm, 96-4, 29 cm, 98-4, 27 cm) are given in Table 2.

Sr* (24.25) depends on dissolution effects induced by the presence of organic matter.

The values of Mn* fluctuate by 0.08 and are probably related to variations in physical and chemical properties of the paleoenvironment: volcanic events along the rift and anoxic conditions. D* is small (0.34), suggesting a scarce detritic influence of the clay fraction, principally or almost certainly related to volcanic events in the Walvis Ridge area.

Si* (9.95) is very high at the base of the sedimentary column and progressively decreases from Albian to Co-

Table 3. Geochemical results, Hole 530A.

Sample (level in cm)	SiO$_2$ (%)	Al$_2$O$_3$ (%)	CaO (%)	MgO (%)	Na$_2$O (%)	K$_2$O (%)	TiO$_2$ (%)	Fe$_2$O$_3$ (%)	Mn (ppm)	Zn (ppm)	Li (ppm)	Ni (ppm)	Cr (ppm)	Sr (ppm)	Co (ppm)	Cu (ppm)	Pb (ppm)	V (ppm)	Cd (ppm)
2-2, 32	57.65	15.70	0.47	2.94	2.17	2.89	0.55	8.51	600	142	49	109	137	153	28	37	7	121	1
4-4, 140	23.50	6.73	29.16	1.74	1.42	1.28	0.26	3.36	411	126	37	17	71	1 132	13	24	81	53	2
5-5, 20	36.35	8.41	16.20	1.85	1.85	1.93	1.09	5.00	258	132	41	45	76	611	11	21	34	68	2
6-2, 136	51.55	12.05	4.99	2.39	2.39	2.62	1.48	5.83	237	118	55	41	121	268	6	23	20	89	1
7-4, 121	17.75	4.74	34.72	1.21	1.25	1.14	0.24	2.23	305	73	28	16	53	1 210	7	19	39	63	1
8-5, 7	48.65	10.86	5.29	2.63	2.36	2.59	0.38	7.04	305	133	68	60	105	237	7	31	13	84	0
9-1, 111	41.40	9.73	12.89	2.24	2.06	2.26	0.29	4.93	300	117	57	40	81	526	7	34	32	63	1
10-6, 5	51.05	12.53	2.64	2.90	2.37	3.01	0.71	7.01	274	127	72	59	118	195	6	35	19	105	0
11-5, 32	40.00	10.28	14.20	2.21	1.92	2.47	0.56	5.36	326	118	48	42	81	568	12	27	31	89	1
12-5, 10	54.65	13.11	2.38	2.69	2.37	3.18	0.73	6.22	263	126	70	41	137	184	8	23	17	95	0
13-3, 93	49.30	12.05	5.39	2.50	2.33	2.80	0.65	7.15	342	120	66	84	123	305	9	25	19	89	1
14-3, 64	15.70	4.14	35.89	1.14	1.08	1.01	0.21	2.50	421	75	23	19	41	1 353	10	22	45	53	2
15-5, 105	17.75	4.84	33.81	1.25	1.04	1.20	0.25	2.93	437	73	26	32	48	1 142	13	17	50	53	2
18-5, 43	54.55	15.59	0.47	2.71	1.95	3.73	0.71	8.15	868	126	69	51	103	105	13	41	25	95	0
20-3, 60	53.05	15.59	0.50	2.99	2.12	3.75	0.77	8.94	474	162	91	65	134	100	23	39	22	89	0
21-5, 125	53.75	14.64	0.50	2.83	2.09	3.75	0.75	8.40	789	168	74	88	113	95	22	47	18	111	0
22-4, 85	54.00	14.28	0.47	2.79	1.95	3.72	0.74	8.22	500	137	61	42	122	105	13	38	27	111	0
24-6, 73	56.50	12.53	0.67	2.83	2.43	2.80	0.69	7.72	600	161	50	55	105	116	17	27	15	126	0
26-3, 51	57.00	12.64	0.64	2.90	2.37	2.97	0.73	7.40	347	137	44	38	111	126	11	87	29	100	0
28-5, 25	55.60	14.42	1.00	2.65	2.56	3.88	0.90	7.15	500	151	66	90	158	121	32	77	27	132	0
30-2, 17	56.65	13.23	0.57	2.61	2.44	2.84	0.73	8.15	458	119	35	44	115	137	16	26	27	95	0
32-3, 8	56.95	13.47	0.67	2.72	2.19	3.34	0.76	8.40	384	148	49	47	123	132	19	25	35	84	0
34-6, 66	56.00	14.64	0.60	2.69	2.16	3.61	0.78	9.08	616	162	64	42	114	132	12	26	25	89	0
36-1, 82	57.55	13.58	0.64	2.97	2.07	3.34	0.79	7.86	379	128	53	35	111	137	12	23	25	84	0
37-3, 41	54.05	4.78	1.74	4.10	2.16	3.13	0.54	8.22	779	285	58	68	103	447	16	48	29	84	0
39-2, 83	24.05	12.05	29.09	2.24	0.96	1.20	0.33	3.04	663	138	23	24	47	189	9	25	42	37	2
40-4, 39	16.55	4.36	35.15	1.60	0.78	1.07	0.26	2.39	342	77	24	18	33	621	7	38	51	26	3
41-3, 122	27.90	6.78	25.91	2.15	1.18	1.75	0.40	4.58	342	116	35	42	74	747	9	81	36	42	2
44-2, 44	75.05	7.33	0.44	2.03	1.28	1.87	0.38	4.18	237	116	34	98	82	95	15	16	21	37	0
49,CC	55.50	12.28	1.67	4.02	2.06	3.23	0.84	8.33	489	195	52	55	116	189	17	39	30	95	3
50-4, 90	56.15	12.53	1.84	3.46	2.49	3.57	0.92	7.22	542	213	52	58	97	242	19	77	42	132	0
51-5, 120	72.90	7.67	1.71	1.58	2.02	2.06	0.43	3.65	232	167	27	13	61	184	3	26	25	26	0
53-2, 63	61.30	9.45	3.11	2.86	2.02	2.68	0.80	6.18	221	147	47	48	67	263	17	132	32	168	1
55-5, 63	48.00	6.86	14.87	2.10	1.38	2.02	0.52	4.11	263	139	38	32	62	326	14	39	41	74	1
57-2, 68	58.85	9.69	4.08	3.32	2.04	3.01	0.84	6.97	253	147	62	32	79	237	11	21	26	100	0
59-2, 24	65.40	9.69	2.75	2.30	2.56	2.62	1.13	5.47	316	122	34	19	122	247	5	20	28	105	0
62-4, 63	48.55	8.03	13.59	2.40	1.45	2.09	0.38	4.47	689	192	33	31	58	326	12	121	51	89	1
64-2, 118	52.65	9.69	6.36	3.40	1.93	2.70	0.88	8.29	442	116	31	50	80	284	22	30	31	158	0
68-5, 30	49.50	6.86	13.83	1.82	1.36	1.60	0.84	5.50	947	118	26	36	58	295	15	49	45	84	1
70-2, 57	48.05	8.62	12.05	2.14	1.75	2.26	0.83	6.79	832	118	23	44	57	368	23	206	40	89	1
72-2, 54	49.25	10.64	5.02	3.48	1.82	4.62	1.36	10.87	647	96	13	96	64	253	30	78	29	211	0
74-2, 28	28.60	5.00	21.55	3.29	1.75	0.27	1.75	10.01	2 484	191	30	47	63	347	32	83	12	226	1
76-1, 102	55.30	9.19	1.05	2.83	2.49	0.30	—	6.72	58	126	17	106	236	437	96	89	40	256	0
78-4, 59	39.25	4.19	16.02	3.67	1.31	1.75	0.79	9.36	2 237	140	20	65	68	289	27	2	13	185	0
79-5, 9	52.25	7.31	6.09	2.47	2.14	1.45	1.83	8.26	284	171	19	58	59	447	23	90	17	168	0
81-1, 119	32.95	3.25	18.26	5.91	1.18	1.45	0.75	8.36	2 658	142	15	45	46	247	29	2	13	94	0
82-5, 114	57.55	5.75	5.46	2.11	1.69	2.65	0.52	8.94	284	168	30	62	77	321	12	12	25	114	0
84-2, 21	49.00	5.81	9.48	2.47	1.85	2.65	1.23	9.11	563	127	34	73	85	395	13	63	29	111	0
86-1, 18	42.15	5.26	10.88	4.61	1.45	2.65	0.92	9.29	2 500	153	21	66	59	279	28	24	40	106	1
87-4, 67	57.65	7.23	0.70	2.88	2.07	3.67	1.46	9.01	537	116	30	144	123	226	21	68	27	184	0
88-2, 114	48.45	6.38	8.92	2.38	1.55	3.34	0.99	9.29	2 537	123	26	46	81	311	11	32	35	129	0
89-4, 52	56.85	7.25	0.73	2.59	1.72	3.91	1.36	10.51	1 579	232	28	74	111	200	16	53	36	174	0
90-3, 28	57.90	7.22	0.84	2.96	1.73	3.61	1.23	7.72	3 500	112	31	98	100	200	55	109	29	188	0
91-2, 89	48.65	5.94	6.72	4.20	1.45	3.01	1.06	7.65	4 500	162	25	49	74	195	16	18	35	127	0
93-5, 26	59.36	6.72	0.70	2.59	1.69	3.22	1.21	7.15	463	271	30	143	147	211	141	208	31	297	0
94-1, 43	38.95	4.31	0.87	1.99	1.23	2.26	0.80	15.23	453	1 500	26	562	212	132	323	375	34	858	7
95-4, 100	63.20	6.53	0.59	2.67	1.72	3.01	1.19	7.65	311	129	37	51	97	179	19	139	22	221	0
96-4, 29	59.50	6.13	0.80	2.66	1.67	2.77	1.23	8.58	268	232	36	88	166	174	35	121	17	321	0
98-4, 27	52.55	5.59	0.56	2.67	1.55	3.46	1.08	13.26	347	375	31	206	242	132	158	132	43	253	0
99-5, 91	66.75	6.06	0.45	2.74	1.38	2.98	0.99	7.51	379	181	32	28	72	121	5	63	12	128	0
100-1, 129	58.70	5.31	5.39	2.87	1.09	2.86	0.71	8.79	2 747	163	27	43	54	158	14	42	19	100	0
102-6, 32	64.70	5.59	0.77	3.01	1.11	2.96	0.88	9.54	968	90	20	44	65	105	8	67	8	117	0
103-4, 121	56.80	3.63	11.26	2.21	0.81	1.83	0.48	5.15	4 000	92	34	15	39	242	5	34	21	74	0
104-3, 51	66.35	5.29	1.33	2.98	1.17	2.80	0.83	6.43	574	111	37	22	56	116	5	53	18	107	0
105-4, 76	62.75	5.66	0.63	2.78	1.60	3.49	1.50	8.04	621	100	44	41	64	137	16	60	24	130	0

niacian times. Fe* is close to 1.55 and Mg* is approximately 0.48. Sr* (4.04) is relatively small in Cores 103, 100, 91, and 88 and large (24.25) in the black shales. This trend can be explained by variations in the anoxicity of the black-shale environment.

From Coniacian-Santonian to Campanian (Cores 530A-86 to 76), calcareous components increase in the sediment: SiO_2, 46.92%; CaO, 9.61%. Mn* values fluctuate considerably above −0.11. D* maintains values (0.31) close to its Albian/Coniacian record, which probably expresses a volcanic influence on the sedimentation.

Si* (8.45) decreases slightly, while Mg* (0.72) and Fe* (−1.65) maintain high values.

Sr* (3.85) decreases progressively and reaches values which are common in marine carbonates.

During the late Campanian (Cores 530A-74 to 64), Mn* values fluctuate strongly above 0.06 and D* increases progressively (0.43). The sediment is characterized by both detrital and volcanic components. The volcanic influence decreases above Core 64.

Si* (5.71), Mg* (0.37), and Fe* (1.09) decrease progressively. The presence of glauconite in the sediment may cause the increase of Fe* (74.2 to 72.2). Sr* maintains values common in marine carbonates.

From late Campanian to the Pliocene (Cores 530A-62 to 2) D* is high (0.56), suggesting an increased influence of terrigenous components. Mn* fluctuates between positive and negative values in response to the lack of an oxidizing environment.

The values of Si* (4.80) suggest a clay mineral assemblage. Sr* values increase in the early Paleocene (Core 50, Section 9), at the top of the middle Paleocene (Core 44), from the middle Eocene to the top of the middle Miocene (Core 20, Section 4), and in the late Pliocene (Core 2, Section 2). These high values indicate that the area was affected by seafloor subsidence or by a rise in the CCD.

In the Pleistocene (Hole 530B, Core 27, Section 2 to Core 2, Section 1) Mn* values are close to those found in samples from late Campanian/Pliocene (−0.08) and result from the lack of bottom oxidation. The excess of silica (SiO_2 = 11.78) is certainly related to the presence of siliceous microfossils. Sr* values fluctuate considerably in the cores. When Sr* is low (Core 44, Section 2 to Core 27, Section 2; Core 25, Section 2 to Core 22, Section 3; and Core 12, Section 2 to Core 2, Section 1), it characterizes marine carbonates devoid of dissolution processes. When Sr* is high (Core 26, Section 2: Sr* = 10.91; Core 20, Section 2 to Core 16, Section 2: Sr* = 17.03), it is typical of dissolved marine carbonates (subsidence or a rise in the CCD).

WALVIS RIDGE, HOLES 532, 532B

Lithology (Fig. 3)

The dominant lithologies are nannofossil ooze, marl, and clay and diatom sarl and smarl.

The bottom of the recovered section is represented by nannofossil marl, the middle part of the section consists of nannofossil diatom marl and sarl, and the top of the section is represented by nanno-foraminiferal and foram-nannofossil ooze and marl.

Clay Mineralogy (Fig. 3)

From late Miocene until late Pleistocene, the composition of the clay assemblage appears relatively homogeneous. Clay minerals include chlorite (trace amounts to 5%), illite (5 to 40%), mixed layers (trace amounts to 25%), smectite (20 to 85%), kaolinite (trace amounts to 10%), and palygorskite (0 to trace amounts). Quartz and feldspar are also present. Fluctuations are present in the relative abundances of these minerals. The composition of the clay minerals assemblage depends mainly on climatic conditions during the late Cenozoic climate cooling.

Geochemistry (Fig. 3 and Table 4)

From late Miocene to Pleistocene, the chemical composition of the sediment appears homogeneous. Mn* (−0.25) shows a regular decrease from −0.17 to −0.25 and increases slightly during the Pleistocene (−0.31). D* (0.58) is close to the values characteristic of terrigenous shales. Si* (4.50) values typical of clay minerals reflect the increased influence of diatoms (Si* = 6.30) on sedimentation during late Pliocene and early Pleistocene.

Despite important lithologic variations (see Table 4) the chemical indices suggest that the paleoenvironment was always detrital and with low concentrations of transition elements. Sr* is very close to the values recorded in marine carbonates where dissolution is absent.

INFLUENCE OF VOLCANISM

Geochemical data point to the presence of a strong volcanic influence in Albian to Santonian sediments at Site 530. Contrary to observations made in other regions of the South Atlantic (Maillot, 1980; Maillot and Robert, 1980; Maillot and Robert, in Debrabant et al., 1981), metallization does not increase in the sediment, because of the presence of an euxinic environment acting against precipitation of metallic oxides. D* is a very close to the values recorded in volcanogenic clay species (Wedepohl, 1978). Clay mineralogical data show that smectite abundance does not increase significantly toward the bottom of the Hole 530A, where the sediment is in contact with the basalt. Generally, oceanic volcanogenic smectite is present a few centimeters above the basalt (Maillot and Robert, in Debrabant et al., 1981), but subaerial alteration of basalts can produce abundant smectite during a long period, as is the case on the Walvis Ridge during the Late Cretaceous (Chamley et al., in press). If one considers the location of Site 530, it appears that a part of the smectite present in Albian to Santonian sediments is volcanogenic, and the other part is possibly produced from removal of subaerial alteration of basalts on Africa or Walvis Ridge. However, the dominant part of the clay mineral assemblage, including smectite, seems to be from pedogenic origin, as suggested by the shape of the X-ray diffractograms.

During Oligocene and early Miocene times, the occurrence of clays rich in volcanogenic components and con-
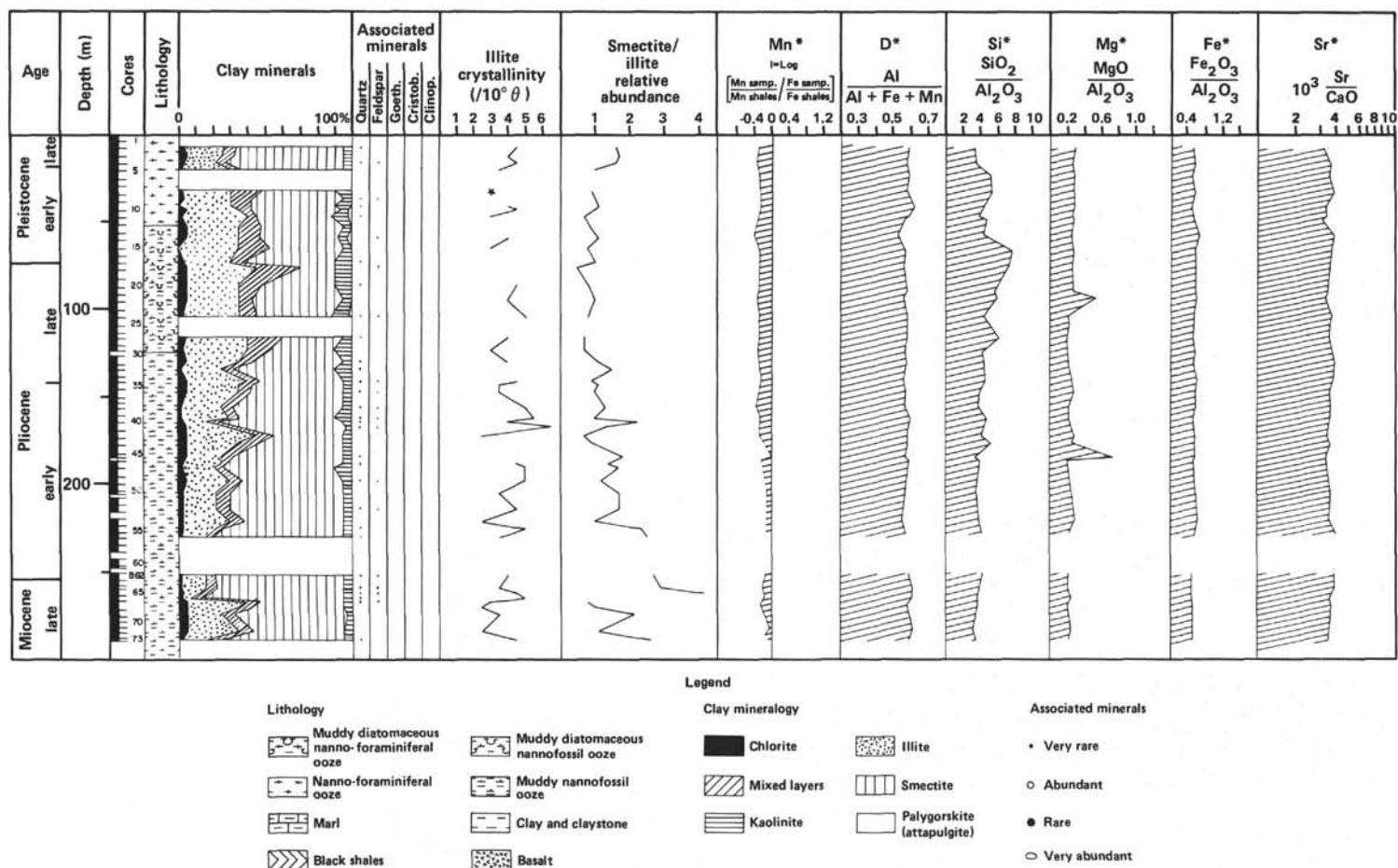
Figure 3. Lithology, geochemistry, and clay mineralogy, Site 532.

Table 4. Geochemical results, Site 532.

Sample (level in cm)	SiO2 (%)	Al2O3 (%)	CaO (%)	MgO (%)	Na2O (%)	K2O (%)	TiO2 (%)	Fe2O3 (%)	Mn (ppm)	Zn (ppm)	Li (ppm)	Ni (ppm)	Cr (ppm)	Sr (ppm)	Co (ppm)	Cu (ppm)	Pb (ppm)	V (ppm)	Cd (ppm)
Hole 532																			
2-3, 86	17.25	5.18	31.20	1.48	1.83	1.20	0.26	2.68	116	288	47	62	97	995	7	44	35	65	2
4-3, 105	22.90	6.41	25.36	1.71	2.02	1.51	0.31	3.54	142	147	38	56	89	916	5	23	16	49	2
6-2, 52	25.00	4.78	25.61	1.39	2.26	1.17	0.23	2.50	116	124	33	65	74	895	3	47	17	51	2
8-2, 104	29.90	5.69	17.73	1.60	2.07	1.37	0.31	3.15	147	115	39	64	95	684	4	34	15	54	2
10-3, 55	21.50	4.82	31.48	1.33	1.65	1.16	0.23	2.25	111	789	29	55	68	1 042	6	19	28	37	3
11-3, 147	24.40	6.44	22.74	1.62	2.07	1.58	0.31	3.32	147	118	52	72	89	768	4	59	25	60	3
12-1, 80	28.10	6.01	25.19	1.60	2.00	1.45	0.30	3.47	147	551	45	72	92	784	5	33	26	52	3
14-2, 33	38.20	8.75	11.47	2.18	2.36	2.14	0.46	5.79	205	155	70	98	108	447	2	81	18	74	2
16-1, 116	29.35	3.85	26.97	1.06	2.12	1.02	0.20	2.14	95	82	25	51	68	984	1	25	26	41	3
18-2, 106	41.50	5.72	17.07	1.49	2.49	1.55	0.29	3.32	147	100	39	55	68	611	1	42	24	52	2
21-3, 77	26.80	4.69	28.26	1.25	1.82	1.20	0.24	2.54	116	78	27	31	55	979	6	21	39	53	1
22-2, 141	31.80	5.31	20.11	2.93	2.01	1.42	0.26	3.15	132	101	33	52	56	674	3	40	24	57	1
24-3, 80	33.05	7.50	18.40	1.60	2.01	1.88	0.35	4.11	200	109	45	52	83	684	4	53	63	74	1
25-2, 48	35.35	6.97	18.92	1.50	2.02	1.79	0.34	3.75	168	100	42	39	66	674	4	33	21	63	1
27-2, 130	43.60	7.09	14.97	1.45	2.12	1.82	0.33	3.79	179	95	44	28	66	526	1	31	13	59	2
29-3, 19	35.80	8.50	14.69	1.81	2.19	2.16	0.42	4.83	205	125	61	64	97	547	5	68	21	79	1
31-3, 15	26.70	6.03	26.72	1.31	1.58	1.51	0.29	3.22	153	1 370	37	41	88	1 021	7	24	23	54	2
34-2, 51	32.90	7.29	19.17	1.84	1.87	1.88	0.42	4.29	184	124	48	73	114	721	6	44	16	65	1
36-1, 69	23.35	5.86	28.51	1.67	1.53	1.51	0.30	3.32	158	106	35	43	80	1 021	7	27	16	57	2
38-2, 36	29.40	7.77	21.72	1.70	1.62	1.93	0.35	4.47	179	256	44	59	98	784	6	45	9	74	1
40-2, 48	28.60	6.01	26.76	1.33	1.65	1.87	0.44	3.04	163	141	49	66	111	953	7	45	26	71	1
42-2, 82	23.45	5.65	29.98	1.59	1.35	1.43	0.28	3.11	147	200	32	30	60	1 021	11	19	8	51	2
43-2, 77	20.65	3.97	32.36	1.04	1.50	1.01	0.19	2.14	132	77	23	32	53	1 158	9	21	24	51	3
45-2, 39	14.20	4.14	33.23	3.03	1.15	1.05	0.18	2.32	211	71	25	15	49	1 105	8	8	17	55	3
46-2, 46	31.90	8.09	20.29	1.69	1.43	1.48	0.29	4.29	189	407	39	33	77	789	9	18	13	63	2
50-1, 6	21.85	6.25	29.63	1.53	1.36	1.51	0.31	3.57	247	378	36	33	77	1 074	11	21	24	65	2
54-1, 87	11.05	2.93	40.23	0.84	1.15	0.72	0.15	1.82	126	83	19	29	46	1 442	5	18	16	42	3
56-2, 24	27.05	6.44	25.33	1.50	1.45	1.61	0.35	3.65	242	136	49	44	82	1 021	9	33	11	77	2
Hole 532B																			
62-1, 120	27.05	6.33	26.24	1.38	1.33	1.48	0.34	3.32	205	163	43	35	71	1 021	8	25	21	68	2
64-2, 14	23.35	5.88	29.56	1.26	1.33	1.33	0.31	2.82	158	184	36	25	65	1 168	7	18	38	62	3
66-1, 69	21.60	5.91	30.78	1.48	1.16	1.22	0.28	2.79	174	68	36	24	58	1 126	7	10	24	62	2
67-2, 51	26.45	7.07	25.47	1.48	1.42	1.55	0.33	3.79	189	102	43	48	67	953	7	44	22	95	3
71-2, 83	11.05	3.46	40.23	0.82	1.06	0.78	0.15	1.68	126	418	19	23	43	1 432	6	17	24	39	3
73-2, 20	1 570	4.50	35.68	0.99	1.08	1.02	0.27	2.36	132	78	28	30	54	1 247	7	20	16	59	3

taining 95 to 100% of well-crystallized smectite in two samples leads to the same conclusion. Here, volcanic particles do not influence the variations of the geochemical indices in an important manner.

CHARACTERS OF EUXINIC SEDIMENTS

Black Shales

At Site 530, the base of the sedimentary column consists of a late Albian black-shale facies overlying an oceanic basalt and a clay assemblage including abundant well-crystallized smectite. This sedimentary facies extends to the Coniacian-Santonian. There is no close relation between the variations of clay minerals, lithology, and organic matter. These data differ from results obtained on Mediterranean sapropels, where decreases in palygorskite or smectite, as well as corrosion of phyllite particles, occur (Sigl et al., 1978). As a consequence, the deposition environment of black shales is characterized by diagenesis of clay minerals, as observed in other regions of the South Atlantic (Robert et al., 1979; Robert and Maillot, in press). As there is no preponderant influence of volcanism on clay minerals at Site 530, the great abundance of smectite expresses primarily the morphology of continental coastal areas. It is suggested that, during late Albian, the region of Site 530 was in the vicinity of flat continental lowlands, where deep gray soils developed on both the African continent and Walvis Ridge, emergent for the most part. These implications are consistent with the results previously

obtained at Site 363 on the Walvis Ridge (Robert et al., 1979) and suggest that the entire area under consideration was tectonically passive by this epoch.

The sediments deposited from Albian to Coniacian-Santonian are also characterized by strong abundances of Cu, Ni, Zn, Co, Cr, and V, in agreement with data obtained at Sites 363 and 364 on the Walvis Ridge and in the Angola Basin (Maillot, 1980).

Late Cenozoic Organic Sediments

Occurrences of organic matter are present at Sites 530 and 532 from Late Miocene to late Pleistocene. The abundance increases progressively from the late Miocene to the end of early Pliocene, and then decreases (Meyers, Brassell, Huc, this vol.). With respect to clay minerals, abundances of chlorite, illite, and mixed layers increase then decrease contemporaneously with the general trend of organic matter accumulations. During the same period, metallization effects are very weak. Oxygen deficiency in the environment probably prevented the precipitation of any metallic oxide. The abundance of organic carbon, depending on planktonic productivity, increased with the development of the Benguela upwelling system during the late Miocene (Diester-Haass and Schrader, 1979; Siesser, 1980). Probably starting during early Oligocene (Peypouqet and Benson, in preparation), the intensity of this upwelling increased as a result of climatic cooling, which led to the development of the Antarctic ice-sheet and oceanic circulation. Thus, organic matter, as well as illite and mixed

layers, which express global climatic and oceanic variations, are more abundant at the end of the early Pliocene, a time when the Antarctic ice sheet reached its greatest extension (Mercer, 1978). Moreover, chlorite, illite, and mixed layers in the oceanic areas subjected to the Benguela system could originate in large part from erosional processes in the relatively arid southwest Africa, as shown by Diester-Haass and Chamley (1980) for sediments along the arid coast of northwest Africa.

TECTONICS AND SUBSIDENCE

From Santonian to late Eocene, increases in the amounts of illite and palygorskite point to the importance of erosion of altered rocks and moderate weathering, as well as of confined coastal basins. Clay mineralogical variations suggest the presence of a continental topography rejuvenated by tectonism, during a period when marginal tectonic events are present all around the Atlantic Ocean, in relation to changes in the direction of ocean opening and increases in the velocity of spreading (Sibuet and Mascle, 1978; Chamley and Robert, 1979). The marginal tectonic activity induces the erosion and removal of elements originating from the continental shelf (i.e., glauconitic sediments), confined coastal basins (i.e., palygorskite), flat downstream lowlands (i.e., smectite), and continental reliefs (i.e., illite and mixed layers). Close to Site 530, in the Rio Grande Rise and Walvis Ridge areas (Robert, 1981, Maillot and Robert, in press), tectonic events, as well as development and removal of semienclosed confined basins appear more influential on sedimentation. They are related to the progressive subsidence of these oceanic barriers and to the deepening of the seafloor, and then disappear when the structures become almost totally submerged.

INFLUENCES OF CLIMATE, CURRENTS, AND DISSOLUTION OF CARBONATES

Following the Cenozoic occurrences of volcanic claystone, the Miocene to Pleistocene sedimentary column shows an irregular increase in chlorite, illite, and mixed layers. This evolution is a consequence of climatic cooling, which was responsible for the progressive diminution in the intensity of weathering on the continents. As a consequence, the abundance of smectite decreases, while chlorite, illite, and mixed layers become abundant (Chamley, 1979). These minerals are slightly more abundant at Site 532, located at a shallower depth than at Site 530. This difference recalls the observations made on sediments from Leg 74 (Maillot and Robert, in press). Site 532 is more strongly subjected to the Benguela current system, which favors the northern transport of detrital components issued from higher latitudes (Robert, 1980); illite and mixed layers principally.

Previous studies on sediments from the Walvis Ridge recovered during Leg 40 (Maillot, 1980; Maillot and Robert, 1980) have shown that a break occurred in the geochemical index Mn* during the middle Miocene. Below, the sedimentary column contains abundant transitional elements high Mn* and above it is poor in these elements low Mn*. The Mn* index is also low in the upper Miocene to Pleistocene section at Site 532 (Fig. 3)

and points to a diminution in the oxygen content of oceanic waters, related to the influence of the oxygen-minimum layer or intermediate waters.

At Site 530, variations in the dissolution of carbonates are present in the sediments. From Albian to Coniacian, dissolution is favored by the presence of organic matter and does not depend on the paleodepth of the site. From Coniacian-Santonian to late Campanian, the sediments are not subjected to dissolution effects. Dissolution episodes occur in the upper Maestrichtian to lower Paleocene, middle Paleocene, and middle Eocene to middle Miocene parts of the section. They are caused by a rise in the CCD, as suggested by previous studies (van Andel et al., 1977; LePichon et al., 1978). The last episode of a dissolution occurred during the late Pliocene and corresponds to a local event, as shown during the same period on the Walvis Ridge (Maillot and Robert, in press).

CONCLUSION

Data obtained by clay mineralogical and inorganic geochemical investigations permit placing the information contained in the sediments recovered during the Leg 75 into the general evolution of the South Atlantic. Data permit the determination of the Cretaceous environment of black-shale deposition, as well as the climatic and morphologic conditions of the continental margins. At the end of the Cretaceous, sediments at Site 530 were influenced by tectonic events and modifications of continental morphology on the African margins and Walvis Ridge, when the ocean width and depth increased. During the Cenozoic, the oceanic environment in this region was marked principally by current-related events; increases in current velocity, existence of upwelling, and dissolution events are related to global climate cooling.

REFERENCES

Bausch, W. M., 1968. Recent developments in carbonate sedimentology in Central Europe. *In Outlines of Distribution of Strontium in Marine Limestones*, Müller, G., and Friedman, G. M. (Eds.), Berlin (Springer-Verlag), pp. 106–115.
Boström, K., 1970. Submarine volcanism as a source of iron. *Earth Planet. Sci. Lett.*, 9:348–384.
Boström, K., Joensuu, O., Valdes, S., Charm, W., and Glacum, R., 1976. Geochemistry and origin of East Pacific sediments sampled during DSDP Leg 34. *In Yeats, R. S., Hart, S. R., et al., Init. Repts. DSDP*, 34: Washington (U.S. Govt. Printing Office), 559–574.
Boström, K., Joensuu, O., Valdes, S., and Riera, M., 1972. Geochemical history of South Atlantic Ocean sediments since Late Cretaceous. *Mar. Geol.*, 12:85–121.
Boström, K., and Peterson, M. N., 1969. The origin of the aluminum poor ferromanganoan sediments in areas of high heat flow in the East Pacific Rise. *Mar. Geol.*, 7:427–447.
Chamley, H., 1979. North Atlantic clay sedimentation and paleoenvironment since the late Jurassic. *In Talwani, M., Hay, W., and Ryan, W. B. F. (Eds.), Deep Drilling Results in the Atlantic Ocean:*

Continental Margins and Paleoenvironment: Washington (Am. Geophys. Union) Maurice Ewing Series, 3:342–360.

Chamley, H., Maillot, H., Duee, G., and Robert, C., in press. Paleoenvironmental history of the Walvis Ridge at the Cretaceous–Tertiary transition from mineralogical and geochemical investigations, *In* Moore, T. C., Jr., Rabinowitz, P. D., et al., *Init. Repts. DSDP,* 74: Washington (U.S. Govt. Printing Office).

Chamley, H., and Robert, C., 1979. Late Cretaceous to early Paleocene environmental evolution expressed by the Atlantic clay sedimentation. *In* Christensen, W. K., and Birkelund, T. (Eds.), *Cretaceous–Tertiary Boundary Events Symposium:* Copenhagen, 2:71–77.

_____, 1982. Paleoenvironmental significance of clay deposits in Atlantic black shales. *In* Schlanger, S. O., and Cita, M. B. (Eds.) *Nature and Origin of Cretaceous Carbon-Rich Facies:* London (Academic Press).

Debrabant, P., Chamley, H., Maillot, H., Robert, C., Leroy, P., and Foulon, J., 1981. Influences continentales et marines lors de l'évolution précoce de l'ocean Atlantique. *Rapp. Ronéot. A.T.P. C.N.R.S,* 4(235).

Diester-Haass, L., and Chamley, H., 1980. Oligocene climatic, tectonic and eustatic history off NW Africa (DSDP Leg 41, Site 369). *Oceanol. Acta,* 3:115–126.

Diester-Haass, L., and Schrader, H. J., 1979. Neogene coastal upwelling history off Northwest and Southwest Africa. *Mar. Geol.,* 29: 39–53.

Dunoyer de Segonzac, G., 1969. Les minéraux argileux dans la diagenèse. Passage au métamorphisme. *Sci. Géol.* (Strasbourg, Mém.), 29:320.

Elderfield, H., 1977. The form of manganese and iron in marine sediments. *In* Glasby, G. P. (Ed.), *Marine Manganese Deposits:* Amsterdam (Elsevier), pp. 269–290.

Frakes, L. A., 1979. *Climates throughout Geologic Time:* Amsterdam (Elsevier).

Goldberg, E. D., and Griffin, J. J., 1964. Sedimentation rates and mineralogy in the South Atlantic. *J. Geophys. Res.,* 69:4293–4309.

Krishnaswami, S., 1976. Authigenic transition elements in Pacific pelagic clay. *Geochim. Cosmochim. Acta,* 40:425–434.

LePichon, X., Melguen, M., and Sibuet, J.-C., 1978. A schematic model of the evolution of the South Atlantic. *Advances in Oceanography:* London (Charnock and Deacon), pp. 1–48.

Maillot, H., 1979. Etude géochimique de la marge Sud-Est et Atlantique (Leg 40 DSDP). *7ème Réun. Ann. Sci. Terre:* Lyon (Soc. Géol. France), p. 306.

Maillot, H., 1980. Géochimie des sédiments crétacés et cénozoïques de la marge Atlantique Sud-orientale (Leg 40 DSDP). *Rev. Géol. Dyn. Géog. Phys.,* 22:75–83.

Maillot, H., and Robert, C., 1980. Minéralogie et geochimie des sédiments crétacés et cénozoïques de l'Ocean Atlantique Sud (marge Africaine, dorsale médio-Atlantique). *Bull. Soc. Géol. France,* 22:777–788.

_____, in press. Paleoenvironment evolution of the Walvis Ridge deduced from inorganic geochemical and clay mineralogical data. *In* Moore, T. C., Jr., Rabinowitz, P. D., et al., *Init. Repts. DSDP,* 74: Washington (U.S. Govt. Printing Office).

Maxwell, A. E., Von Herzen, R. P., et al., 1970. *Init. Repts. DSDP,* 3: Washington (U.S. Govt. Printing Office).

Melguen, M., 1978. Facies evolution, carbonate dissolution cycles in sediments from the eastern South Atlantic (DSDP Leg 40) since the Early Cretaceous. *In* Bolli, H. M., Ryan, W. B. F., et al., *Init. Repts. DSDP,* 40: Washington (U.S. Govt. Printing Office), 981–1024.

Melguen, M., LePichon, X., and Sibuet, J.-C., 1978. Paléoenvironnement de l'Atlantique Sud. *Bull. Soc. Géol. France,* 20:471–489.

Mercer, J. H., 1978. Glacial development and temperature trends in the Antarctic and in South America. *In* Van Zinderen Bakker, E.

M. (Ed.), *Antarctic Glacial History and World Paleoenvironments:* Rotterdam (A. A. Balkema), pp. 73–79.

Millot, G., 1964. *Géologie des Argiles:* Paris (Masson).

Natland, J. H., 1978. Composition, provenance and diagenesis of Cretaceous clastic sediments drilled on the Atlantic continental rise off southern Africa, DSDP Site 361: Implications for the early circulation of the South Atlantic. *In* Bolli, H. M., Ryan, W. B. F., et al., *Init. Repts. DSDP,* 40: Washington (U.S. Govt. Printing Office), 1025–1061.

Nekrassov, B., 1966. *Chimie Minérale: Généralites et Étude des Éléments:* Moscow (Editions de Moscou).

Odin, G. S., and Giresse, P., 1972. Formation de minéraux phylliteux (benthiérine, smectites ferrifères, glauconite ouverte) dans les sédiments du golfe de Guinée. *C. R. Acad. Sci.* (Paris), 275:177–180.

Paquet, H, 1969. Evolution géochimique des minéraux argileux dans les altérations et les sols des climats méditerranéens et tropicaux à saisons contrastées. *Sci. Géol., Mém.* 30. (Strasbourg).

Pedro, G., 1968. Distribution des principaux types d'alteration chimique à la surface du globe. Presentation d'une esquisse géographique. *Rev. Geogr. Phys. Geol. Dyn.,* 10:457–470.

Robert, C., 1980. Climats et courants cenozoïques dans l'Atlantique Sud d'après l'etude des minéraux argileux (Legs 3, 39 et 40 DSDP). *Oceano. Acta,* 3:369–376.

_____, 1981. Santonian to Eocene palaeogeographic evolution of the Rio Grande Rise (South Atlantic) deduced from clay mineralogical data (DSDP Legs 3 and 39). *Paleogeog., Paleoclimatol., Paleoecol.,* 33:311–326.

Robert, C., Herbin, J. P., Deroo, G., Giroud d'Argoud, G., and Chamley, H., 1979. L'Atlantique Sud au Crétacé d'après l'étude des minéraux argileux et de la matière organique (Legs 39 et 40 DSDP). *Oceanog. Acta,* 2:209–218.

Robert, C., and Maillot, H., in press. Paleoenvironmental significance of clay mineralogical and geochemical data, Southwest Atlantic (DSDP Legs 36 and 71). *In* Ludwig, W. J., Krashenninikov, V. A., et al., *Init. Rep. DSDP,* 71: Washington (U.S. Govt. Printing Office).

Sibuet, J.-C., and Mascle, J., 1978. Plate kinematic implications of Atlantic equatorial fracture zone trends. *J. Geophys. Res.,* 83: 3401–3421.

Siesser, W. G., 1980. Late Miocene origin of the Benguela upwelling system off Northern Nannibia. *Nature,* 208:283–285.

Sigl, W., Chamley, H., Fabricius, F., Giroud d'Argoud, G., Müller, J., 1978. Sedimentology and environmental conditions in sapropels. *In* Hsü, K. J., Montadert, L., et al., *Init. Repts. DSDP,* 42, Pt. 1: Washington (U.S. Govt. Printing Office), 445–464.

Trauth, N., 1977. Argiles évaporitiques dans la sédimentation carbonatée tertiaire. Bassins de Paris, de Mormoiron et de Salinelles (France); Jbel Ghassoul (Maroc). *Sci. Geol., Mém.* (Strasbourg), 49.

Turekian, K. K., 1965. Some aspects of the geochemistry of marine sediments. *In* Reilly, J. P., and Skirrow, G. (Eds.), *Chemical Oceanography:* London (Academic Press), 2:81–126.

van Andel, Tj. H., Thiede, J., Sclater, J. G., and Hay, W. W., 1977. Depositional history of the South Atlantic ocean during the last 125 million years. *J. Geol.,* 85:651–698.

Vine, J. D., and Tourtelot, E. R., 1970. Geochemistry of black shales deposits. A summary report. *Econ. Geol.,* 65:253–272.

Wedepohl, K. H., 1978. Manganese: Abundance in common sediments and sedimentary rocks. *Handbook of Geochemistry:* Berlin (Springer-Verlag), pp. 1–17.
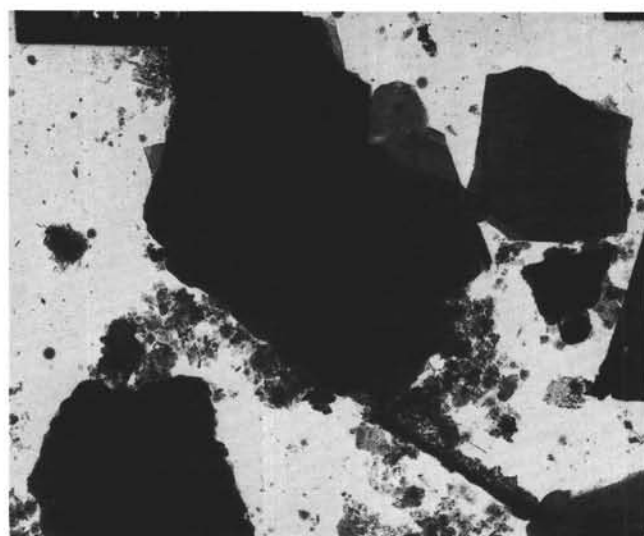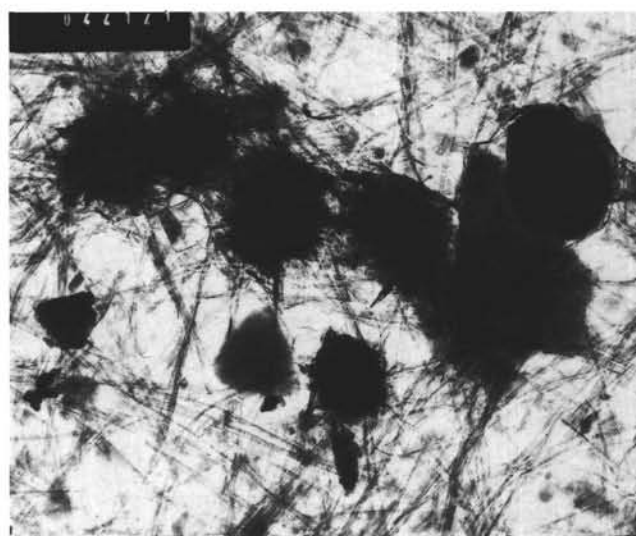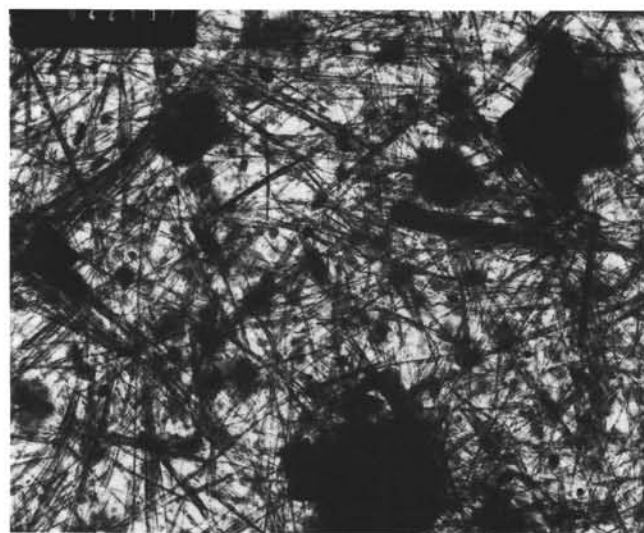
Plate 1. Electronmicrographs. **1.** Sample 530B-22-3, 71 cm ($\times$8,000); early Pleistocene; well-shaped particles of illite, fleecy particles of smectite, and fragments of diatoms. **2.** Sample 530A-39-2, 83 cm ($\times$12,500); early Eocene; palygorskite in long and straight fibers, smectite with blurred contours, and well-shaped illite. **3.** Sample 530A-39-2, 83 cm ($\times$20,000); early Eocene; Palygorskite in long and straight fibers, smectite with blurred contours, and well-shaped illite. (Some fibers appear to grow at the periphery of dense particles.) **4.** Sample 530A-39-2, 83 cm ($\times$40,000); early Eocene; Fibers of palygorskite growing at the periphery of dense particles (detail of Fig. 3).
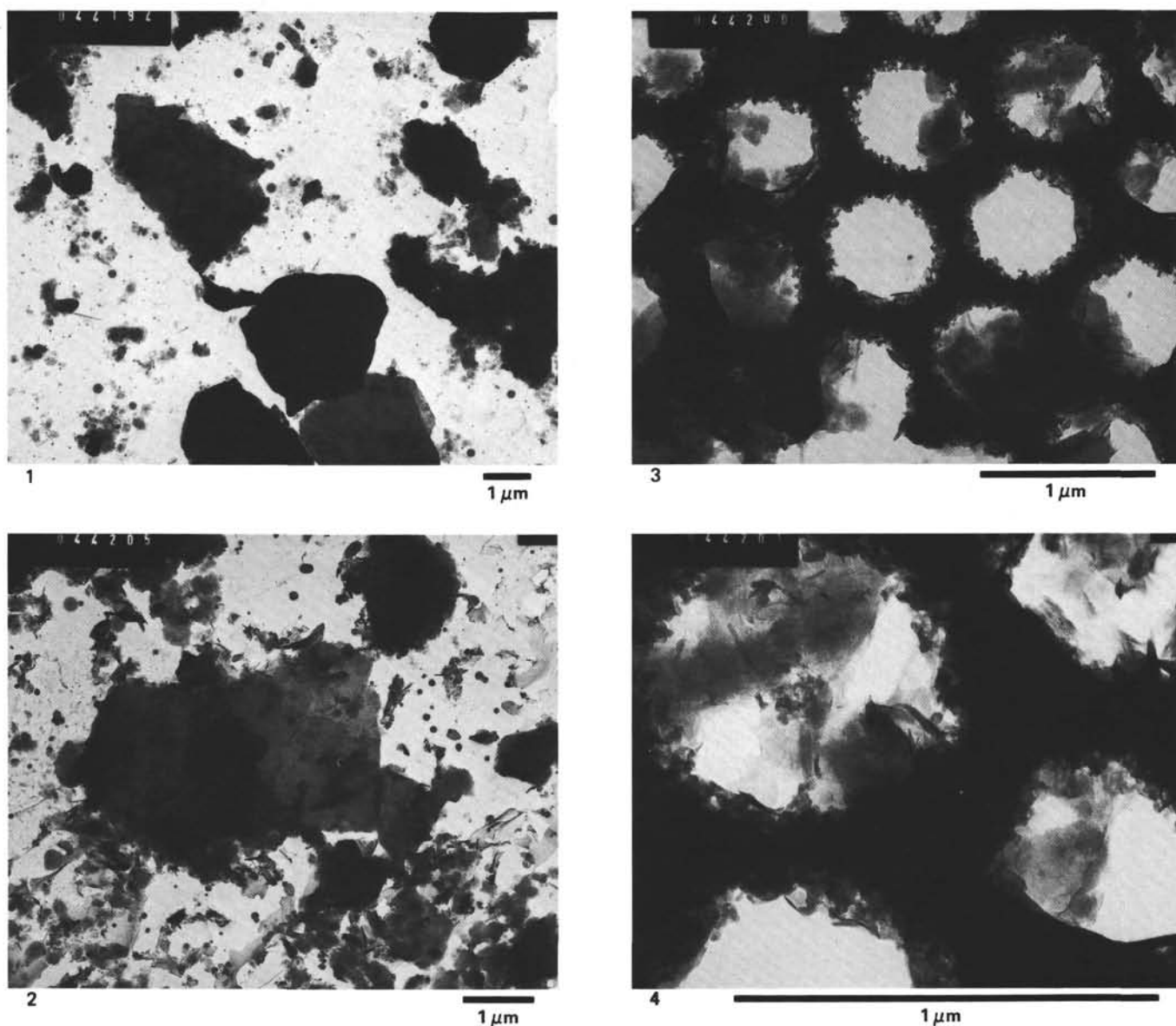
Plate 2. Electronmicrographs. **1.** Sample 532-4-3, 105 cm (×8,000); late Pleistocene; well-shaped particles of illite, small particles of chlorite or kaolinite, and smectite with blurred contours. **2.** Sample 532-56-2, 24 cm (×12,500); early Pliocene; well-shaped particles of illite, smectite with blurred contours, and fragments of diatoms. **3.** Sample 532-15-3, 40 cm (×31,500); early Pleistocene; fragment of diatom with traces of dissolution, and clay particles with blurred contours, probably smectite. **4.** Sample 532-15-3, 40 cm (×75,000); early Pleistocene; fragment of diatom with traces of dissolution and clay particles with blurred contours or in short fibers, probably smectite (detail of Fig. 3).